

## Original Article

# Magnetic resonance imaging monitoring therapeutic response to dendritic cell vaccine in murine orthotopic pancreatic cancer models

Liang Pan<sup>1,2\*</sup>, Na Shang<sup>2\*</sup>, Junjie Shangguan<sup>2</sup>, Matteo Figini<sup>2</sup>, Wei Xing<sup>1</sup>, Bin Wang<sup>3</sup>, Chong Sun<sup>4</sup>, Jia Yang<sup>2</sup>, Yaqi Zhang<sup>2</sup>, Su Hu<sup>2</sup>, Quanhong Ma<sup>2</sup>, Jian Wang<sup>2,5</sup>, Yury Velichko<sup>2,6</sup>, Vahid Yaghmai<sup>2,6</sup>, Al B III Benson<sup>6,7</sup>, Zhuoli Zhang<sup>2,6</sup>

<sup>1</sup>Department of Radiology, Third Affiliated Hospital of Soochow University, Changzhou 213003, Jiangsu, China;

<sup>2</sup>Department of Radiology, Feinberg School of Medicine, Northwestern University, Chicago 60611, IL, USA;

<sup>3</sup>Department of Surgery, Second Affiliated Hospital, Zhejiang University School of Medicine, Hangzhou 310009, Zhejiang, China; <sup>4</sup>Department of Orthopedics, Affiliated Hospital of Qingdao University, Qingdao 266005, Shandong, China; <sup>5</sup>Department of Radiology, Southwest Hospital, Third Military Medical University, Chongqing 400038, China; <sup>6</sup>Robert H. Lurie Comprehensive Cancer Center, Chicago 60611, IL, USA; <sup>7</sup>Department of Hematology and Oncology, Feinberg School of Medicine, Northwestern University, Chicago 60611, IL, USA. \*Equal contributors.

Received January 23, 2019; Accepted February 18, 2019; Epub March 1, 2019; Published March 15, 2019

**Abstract:** Pancreatic ductal adenocarcinoma (PDAC) carries the worst prognosis and caused one of the highest cancer-related mortalities. Dendritic cell (DC) vaccination is a promising cancer immunotherapy; however, the clinical outcomes are often poor. The administration route of DC vaccine can significantly alter the anti-tumor immune response. Here we report on the cytotoxic T lymphocyte (CTL) responses induced by DC vaccination administered via intraperitoneal (IP) for murine PDAC, and the longitudinal assessment of tumor growth and therapeutic responses using magnetic resonance imaging (MRI). In this study, we established murine orthotopic Panc02 models of PDAC and delivered apoptotic Panc02 cell-pulsed DCs via IP injection. The migration of Panc02-pulsed DCs into spleens significantly increased from 6 h to 12 h after initiation of treatment ( $P = 0.002$ ), and Panc02-pulsed DCs injected via IP induced a significantly higher level of CTL responses against Panc02 cells compared to unpulsed DCs. Tumor size and tumor apparent diffusion coefficient (ADC) were measured on MR images. Tumor sizes were significantly smaller in the treated mice than in the untreated mice ( $P < 0.05$ ). The reduction of tumor ADC was less in the treated mice than in the untreated mice ( $P < 0.05$ ), and the changes in tumor ADC showed significant negative correlation with the changes in tumor volume ( $r = -0.882$ , 95% confidence interval,  $-0.967$  to  $-0.701$ ,  $P < 0.0001$ ). These results demonstrated the efficacy of DC vaccination administered via IP injection in murine PDAC, and the feasibility of ADC measurement as an imaging biomarker for assessment of therapeutic responses in immunotherapy.

**Keywords:** Pancreatic ductal carcinoma, dendritic cell, vaccination, intraperitoneal injection, magnetic resonance imaging

## Introduction

Pancreatic ductal adenocarcinoma (PDAC) accounts for over 95% of all pancreatic malignancies. The 5-year survival rate is approximately 7.1% and the median overall survival (OS) is 4-6 months for all patients with PDAC [1, 2]. Surgical resection, the only potentially curative treatment, is applicable in only 5% to 25% patients; even after surgery, the 5-year survival rate is less than 20% [3]. Local ablation and systemic chemotherapy have offered little benefit [4]. Thus, new approaches are

urgently needed to treat this deadly disease effectively.

Recently, many immunotherapies are based on the vaccination of cancer patients with autologous DCs loaded with tumor antigens (DC vaccines) [5-7]. DCs are the main type of antigen-presenting cells (APCs), and the aim of DC vaccination is to induce tumor-specific effector T cells that can specifically reduce the tumor mass and induce immunological memory to control tumor recurrence [8-10]. DC vaccination has clinically relevant mechanisms of action

with a great potential for the systemic treatment of cancers in a clinical setting. However, clinical trials have demonstrated its poor therapeutic efficacy [11-13]. The efficacy of DC vaccination is strongly influenced by DC vaccine migration to the draining lymph nodes (LNs). It has been reported that the administration route of DC vaccine can significantly alter the anti-tumor immune response and immune memory [13, 14]. Administration routes including subcutaneous, intradermal, intratumoral, or intranodal injection have been applied in both preclinical research and clinical trials [15, 16]. However, only a small number of DCs can migrate to LNs and lymphoid organs by subcutaneous or intradermal injection [17, 18]. A direct delivery of DCs by intratumoral injection or by intranodal injection could impair the efficacy of DC vaccine [18, 19]. Given that a large number of LNs in the abdomen composes the most important secondary lymphoid organ and the fact that spleen is the largest lymphatic organ in the abdomen, we have very recently tested the migration of DCs to LNs via intraperitoneal (IP) injection, and the results indicated that IP injection could increase the amount of viable DC vaccines actively absorbed by LNs and improve outcomes.

Magnetic resonance imaging (MRI), which can provide anatomic and functional information about tumors, has a well-established role in the evaluation of patients with PDAC [20]. Diffusion weighted MRI (DW-MRI), which reflects the diffusion of water molecules within biological tissues, provides microstructural information at the cellular level [21, 22]. The apparent diffusion coefficient (ADC), which can be quantified from DW-MRI, decreases when water molecule movements are hindered by any obstacle; in particular, it has been proved to reduce in tissues with high cell density [23]. Studies on a variety of tumor types reported that tumor ADC could act as an imaging biomarker for early detection of cancer treatment response [24-27]. To the best of our knowledge, no studies have assessed DC vaccine therapeutic responses in PDAC using DWI.

The purpose of our study was to test the following hypotheses in a murine model of PDAC: (a) DC vaccines administered via IP injection can effectively induce tumor-specific cytotoxic T lymphocyte (CTL) response and inhibit the growth of PDAC; (b) ADC measurement can offer an imaging biomarker for evaluation

of therapeutic response of DC vaccination in PDAC.

### Materials and methods

Our study was approved by the Institutional Animal Care and Use Committee (IACUC) of Northwestern University.

#### *Cell lines and culture*

The mouse Panc02 cell line is derived from amethylcholanthrene-induced pancreatic ductal adenocarcinoma in C57BL/6 mice and was purchased from the American Type Culture Collection (ATCC; Rockville, MD). Panc02 cells were cultured in RPMI 1640 medium (Life Technologies, Carlsbad, CA) supplemented with glutamine (2 mmol/l, Life Technologies), pyruvate (1 mmol/l, Sigma-Aldrich, St. Louis, Mo), penicillin and streptomycin (100 IU/ml, Sigma-Aldrich), and 10% fetal bovine serum (FBS, Sigma-Aldrich). The cells were maintained in a humidified atmosphere of 5% CO<sub>2</sub> at 37°C. Before implantation, cell viability was assessed using trypan blue (Sigma-Aldrich) staining (cell viability of > 90% was confirmed prior to tumor implantation).

#### *UV-B irradiation of Panc02 cells*

Panc02 cells were diluted in phosphate-buffered saline (PBS) at a final concentration of  $2 \times 10^6$ /ml, and were placed in a 6-well plate at 0.5 ml per well. Panc02 cells were irradiated using UV-B light with 0.75 J/cm<sup>2</sup>. After irradiation, cells were maintained in culture medium. 12 h later, Panc02 cell apoptosis was confirmed by flow cytometric analysis using Annexin V/PI staining (**Figure 1**). The inactivated Panc02 cells were collected for co-incubation with DCs.

#### *Generation and antigen loading of bone marrow-derived DCs*

The mouse bone marrow-derived DCs (BMDCs) were prepared as described in a previous publication with some modifications [28]. Briefly, female C57BL/6 mice (5-6 weeks of age, weighted between 16 and 19 g; Charles River, Wilmington, MA) were sacrificed by CO<sub>2</sub> narcosis and cervical dislocation, and the tibias and femurs were harvested. After immersion in 70% ethanol for 5 mins, the bones were carefully dissected, and each half was flushed with FBS-free RPMI 1640 (Gibco, Waltham, MA) in a cell

## MRI monitoring DC vaccine in murine pancreatic cancer models

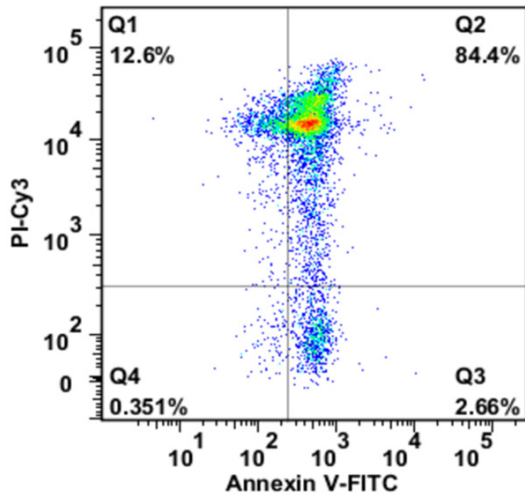


**Figure 1.** Apoptosis in Panc02 cells after UV-B irradiation. 12 hours after UV-B irradiation, apoptosis in Panc02 cells was assessed by flow cytometric analysis using Annexin V/PI staining. The inactivation of all Panc02 cells was confirmed before co-incubation with DCs.

culture hood. The bone marrow cells were collected, and erythrocytes were lysed with ammonium chloride buffer (BD Biosciences, San Jose, CA). A total of  $2 \times 10^6$  cells was cultured in 10 mL RPMI supplemented with 10% FBS (Gibco, Waltham, MA), 100 units/mL penicillin, 100  $\mu\text{g}/\text{mL}$  streptomycin, 0.25  $\mu\text{g}/\text{mL}$  amphotericin b (antibiotic-antimycotic 100  $\times$ , Gibco, Waltham, MA), 10 ng/mL rm-GM-CSF, and 1 ng/mL rm-IL-4 (both from Shenandoah Biotechnology, Warwick, PA). Equal volume of the same culture media was added after 48 h. At day 7, lipopolysaccharide (LPS, 250 ng/ml) and interferon  $\gamma$  (IFN $\gamma$ , 100 ng/ml) were added for 24 h. Loosely adherent cells were then harvested, and the expression of DC markers was analyzed by fluorescence-activated cell sorting (FACS) as described below. BMDCs were co-incubated with the inactivated Panc02 cells at a DC/Panc02 cell ratio of 10:1 for 24 hours. At day 9, loosely adherent cells (Panc02-pulsed DCs) were harvested, washed and resuspended in PBS, and analyzed by FACS.

### FACS

Panc02-pulsed DCs were collected after 8 d of *in vitro* culture and washed with cold PBS. BMDC were stained by incubation for 40 mins at 4°C with 2  $\mu\text{g}/3 \times 10^5$  cells anti-mouse PerCP-Cy<sup>TM</sup>5.5 CD11c monoclonal antibody (mAb), PerCP-Cy<sup>TM</sup>5.5 CD11b mAb, PE CD80

mAb, APC CD86 mAb, PE H2Db mAb, FITC H2Kb mAb (all from BD Bioscience, San Jose, CA), PE MHC class II mAb (Southern Biotech, Birmingham, AL), and appropriate isotype controls. The expression of DC markers was quantified by fluorescence-activated cell sorting (FACS) using flow cytometry (BD LSRFortessa<sup>TM</sup> cell analyzer, San Jose, CA) and analyzed using FlowJo (Ashland, OR).

### Migration of Panc02-pulsed DCs to spleens via IP injection

Migration of Panc02-pulsed DCs to spleens after IP injection was visualized, as spleen is the largest lymphoid organ in the abdominal cavity.  $1 \times 10^7$  Panc02-pulsed DCs in 100  $\mu\text{L}$  Diluent C were mixed with 0.4  $\mu\text{L}$  PKH26 dye in equal volume of Diluent C for 5 mins (Sigma-Aldrich, St. Louis, MO). After adding 200  $\mu\text{L}$  FBS and washing 3 times with PBS, the DCs were labeled with PKH26. Twelve C57BL/6 mice were IP injected with  $1 \times 10^7$  PKH26-labeled Panc02-pulsed DCs in 100  $\mu\text{L}$  PBS. 6 mice were randomly euthanized at each time point (6 h and 12 h after IP injection) to harvest the spleens for fluorescence staining. The collected spleen tissues were embedded in OCT (Fisher HealthCare, Houston, TX) infused modes that were placed on dry ice and frozen at -80°C after 2 mins. The frozen samples were cut into 5  $\mu\text{m}$  thick slices with the microtome and placed on slides. Then the slides were mounted by cover glasses with ProLong Glod Antifade Reagent with DAPI (Cell Signaling Technology, Danvers, MA) and visualized by fluorescent microscope (Axioimager Z1, Carl Zeiss, Ontario, CA). Three representative fluorescent microscopy images were acquired from each sample with the same filter settings at the same magnifications. Total cells counts and PKH26 positive cells counts from the fluorescence microscopy images were quantified using ImageJ software (NIH, Bethesda, MD). The ratio of PKH26 positive cells to total number of cells was calculated for each sample.

### Orthotopic mouse model of pancreatic cancer

Female C57BL/6 mice were used for establishing orthotopic pancreatic cancer models. The orthotopic mouse model of pancreatic cancer was prepared using previously published protocols with modifications [29].  $1 \times 10^5$  viable Panc02 cells were gently mixed with ice-cold

## MRI monitoring DC vaccine in murine pancreatic cancer models

Matrigel (Sigma-Aldrich) at a ratio of 3:1 to produce a homogeneous suspension. Anesthesia was induced and maintained in each mouse by inhalation of 2% isoflurane in oxygen at a rate of 1 L/min (Isoflurane Vaporizer, Vaporizer Sales and Services, Rockmart, GA). After local shaving and disinfection, the abdominal cavity was opened by a 1.5-cm longitudinal incision at the left upper quadrant. The tail of the pancreas was identified by mobilization of the spleen. 5  $\mu$ L of PancO2 cell-Matrigel suspension was then slowly injected into the parenchyma of pancreatic tail. To prevent further leakage, the needle was kept in the injection site for 30 s prior to removal. The spleen and pancreas were placed back into the abdominal cavity, and the abdominal cavity was closed by a running two-layer silk suture. Postoperative status and wound healing were monitored every day for one week. After one week, a visible nodule at the location of pancreatic tail was detected by magnetic resonance imaging (MRI) in all eighteen mice (protocols described below), which indicated that the orthotopic pancreatic cancer models were established successfully.

### *Therapeutic strategy*

Twelve mice with orthotopic pancreatic cancer were randomly divided into two groups: treatment group ( $n = 6$ ) and control group ( $n = 6$ ). Therapeutic strategy was started one week after tumor implantation. The mice in the treatment group underwent IP injection of  $1 \times 10^7$  PancO2-pulsed DCs in 100  $\mu$ L PBS for therapeutic vaccination, and the mice in the control group underwent IP injection of 100  $\mu$ L saline solution. IP injection was administered once a week for 5 weeks.

### *CTL assay*

Twelve orthotopic pancreatic cancer mice and six age-matched normal C57BL/6 mice were used for CTL assay. One week after tumor implantation, six of the mice with orthotopic pancreatic cancer were IP injected with  $1 \times 10^7$  PancO2-pulsed DCs in 100  $\mu$ L PBS, and the other six were IP injected with  $1 \times 10^7$  unpulsed mature DCs in 100  $\mu$ L PBS. IP injection was administered once a week for 3 weeks. The six normal C57BL/6 mice that did not undergo any operation were used as another control group. After sacrifice, spleens were harvested and homogenized to release splenocytes in RPMI

1640 medium. The single-cell suspension was prepared, and CD8+ T cells were isolated using magnetic cell sorting by negative selection (CD8a+ T cell isolation Kit, Miltenyi Biotec) according to the manufacturer's instructions. PancO2-pulsed DC-induced, unpulsed DC-induced, and normal murine CD8+ T cells were prepared. Flow cytometry confirmed > 95% purity. Lactate dehydrogenase (LDH) assay was performed to determine the cytotoxicity of the purified CD8+ T cells using Cytotoxicity Detection Kit<sup>PLUS</sup> (Sigma-Aldrich). For LDH assay, PancO2 cells (target cells) were collected and plated at 3000 cells/well in a flat-bottom 96-well cell culture plate (BD Biosciences, San Diego, CA, USA). Then, CD8+ T cells (effector cells) were added to the 96-well plates at different effector-to-target (E:T) ratios (5:1, 10:1, 20:1 and 40:1), and 2% Triton X-100 lysing solution was added to the wells that were prepared for maximal LDH release measurement. The plate was incubated at 37°C for 4 h. After incubation, the plates were centrifuged for 10 min at  $330 \times g$ , and 100  $\mu$ L/well cell-free supernatant was transferred into the corresponding wells of an optically clear, flat-bottom 96-well plate. Then, 100  $\mu$ L mixed detection kit reagent was added to each well, and cells were incubated at room temperature in the dark for 30 min. After incubation, the absorbance was measured using a multiwell plate reader at 490 nm. The percentage of cytotoxicity was calculated according to the following equation: cytotoxicity (%) =  $[(ET - E) - T]/(Max - T) \times 100$ , where *ET* is the LDH release by effector-target reaction, *E* is the spontaneous LDH release of effector cells, *T* is the spontaneous LDH release of target cells, and *Max* is the maximal LDH release from complete target cell lysis.

### *MRI examination*

MRI examinations were performed by using a 7.0 T small-animal MRI scanner with a commercial mouse coil (ClinScan, Bruker Biospin). One week after tumor implantation, all the mice underwent MRI examination to confirm the successful establishment of orthotopic pancreatic cancer models. The mice in the treatment group and the control group underwent MRI examination at one week, three weeks, and five weeks after initiation of treatment for monitoring tumor growth and evaluating the response to therapies *in vivo*. Mice were anesthetized by

inhalation of a mixture of 2% isoflurane and oxygen at 1 L/min, and body temperature was monitored continuously and was controlled with a water bed (SA Instruments, Stony Brook, NY). The MRI sequences and parameters were as follows: (a) axial T1-weighted imaging (T1WI): repetition time (TR)/echo time (TE) = 630/20 ms; field of view (FOV) = 27 mm × 30 mm; matrix size = 134 × 192; slice thickness (ST) = 0.8 mm; gap = 0 mm; (b) axial T2-weighted imaging (T2WI): TR/TE = 1581/40 ms; FOV = 21 mm × 30 mm; matrix size = 180 × 256; ST = 0.8 mm; gap = 0 mm; (c) coronal T2WI: TR/TE = 2500/40 ms; FOV = 23 mm × 32 mm; matrix size = 142 × 192; ST = 0.8 mm; gap = 0 mm; (d) sagittal T2-weighted imaging: TR/TE = 2500/40 ms; FOV = 24 mm × 30 mm; matrix size = 154 × 192; ST = 0.5 mm; gap = 0 mm; (e) axial diffusion-weighted imaging (DWI): TR/TE = 3500/40 ms; FOV = 28 mm × 28 mm; matrix size = 82 × 82; ST = 1 mm; gap = 0 mm; b-value = 0 and 800 s/mm<sup>2</sup>. DWI was performed in 3 orthogonal directions of the diffusion gradients.

### MR image analysis

MR images were analyzed by a radiologist with more than 5 years of experience. *In vivo* tumor size measurement was performed by using an open source software ITK-SNAP (version 3.6.0, University of Pennsylvania) by measuring both the longest diameter and tumor volume. The longest diameter of each orthotopic tumor was measured on either axial, coronal or sagittal T2-weighted images. For tumor volume measurement, free-hand regions of interest (ROIs) were traced along the tumor margin on each slice of axial T2-weighted images containing a orthotopic tumor, and then the three-dimensional volume was calculated [30]. The change in the longest diameter ( $\Delta$ diameter) after five weeks of treatment was calculated according to the equation:  $\Delta$ diameter = diameter<sub>5w</sub> - diameter<sub>1w</sub>, where diameter<sub>1w</sub> and diameter<sub>5w</sub> are the longest diameters that measured at one week and five weeks after initiation of treatment, respectively. The change in tumor volume ( $\Delta$ volume) after five weeks of treatment was calculated according to the equation:  $\Delta$ volume = volume<sub>5w</sub> - volume<sub>1w</sub>, where volume<sub>1w</sub> and volume<sub>5w</sub> are the tumor volumes that measured at one week and five weeks after initiation of treatment, respectively.

Diffusion-weighted images were postprocessed to generate ADC maps in Matlab R2016b (Mathworks, Natick, MA). Using axial T2-weighted images as reference, a free-hand ROI was drawn inside the tumor on the slice of ADC maps with the largest tumor area, avoiding regions with necrosis and artifacts, and the mean ADC for each orthotopic tumor was recorded. The change in tumor ADC ( $\Delta$ ADC) after five weeks of treatment was calculated according to the equation:  $\Delta$ ADC = ADC<sub>5w</sub> - ADC<sub>1w</sub>, where ADC<sub>1w</sub> and ADC<sub>5w</sub> are, respectively, the tumor ADC that measured at one week and five weeks after initiation of treatment.

### Statistical analysis

Statistical analysis was performed using SPSS (version 22.0; SPSS, Chicago, IL). The results are presented as mean ± standard deviation (SD). Mann-Whitney *U* test was applied to compare the difference between the ratio of PKH26 positive DCs to the total cells in the spleens harvested 6 h and 12 h after IP injection. Repeated measures ANOVA analysis was applied to compare the differences in the longest diameter and tumor volume between the treatment and the control group and the changes over time. Student's *t* test was used to compare the differences in  $\Delta$ ADC and  $\Delta$ volume between the treatment group and the control group. The differences in the cytotoxicity between normal, MDI, and PDI CD8+ T cells were determined using One-Way ANOVA analysis followed by *LSD* test for multiple comparisons. Pearson correlation coefficient (*r*) and 95% confidence interval (CI) was calculated to assess the relationship between  $\Delta$ diameter and  $\Delta$ ADC, and the relationship between  $\Delta$ volume and  $\Delta$ ADC. For the absolute value of *r*, 0-0.19 is regarded as very weak, 0.2-0.39 as weak, 0.40-0.59 as moderate, 0.6-0.79 as strong, and 0.8-1.0 as very strong correlation. *P* < 0.05 was considered to indicate a significant difference in all statistical tests.

## Results

### Purity and maturity of bone marrow-derived DCs and Panc02-pulsed DCs

The purities of DCs in BMDCs were analyzed on FACS by assessing the population of cells with positive CD11b and CD11c expression. As shown in **Figure 2**, the population of DCs in

## MRI monitoring DC vaccine in murine pancreatic cancer models

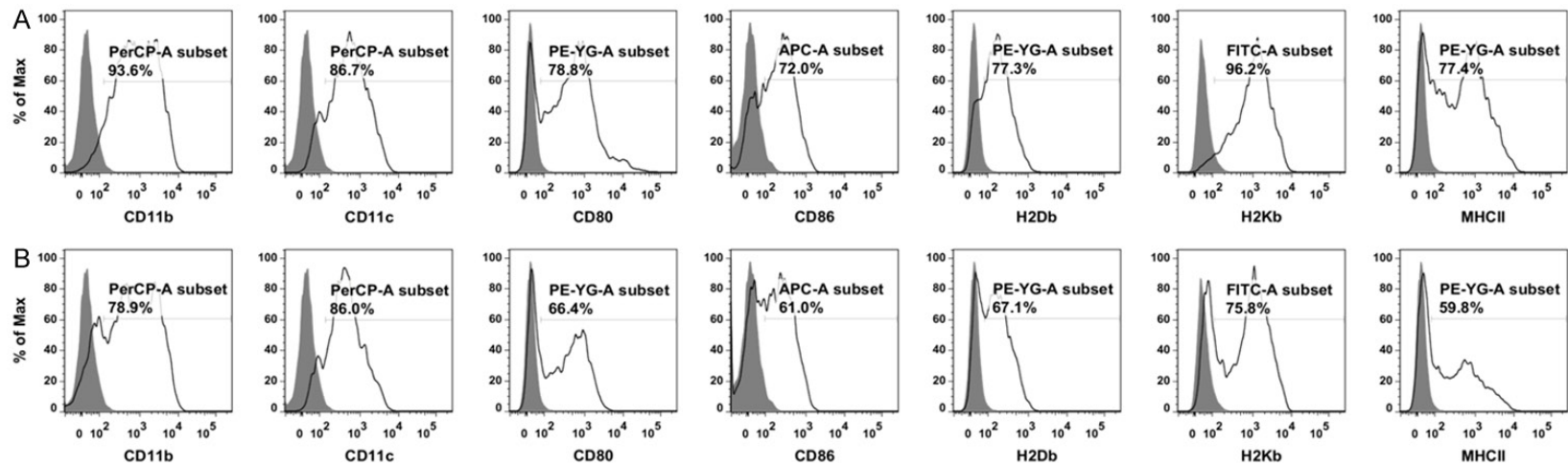


**Figure 2.** The immunophenotypes of bone marrow-derived cells *in vitro* culture for 8 days and PancO2-pulsed DCs. A. The immunophenotypes of bone marrow-derived cells *in vitro* culture for 8 days. B. The immunophenotypes of PancO2-pulsed DCs. The results showed that the purity of CD11b+ DCs and CD11c+ DCs were more than 75% for both bone marrow-derived cells 8 days after *in vitro* culture and PancO2-pulsed DCs. The high expression of the maturation surface markers CD80, CD86, H2Db, H2Kb and MHC class II indicated that the DCs were in a mature state.

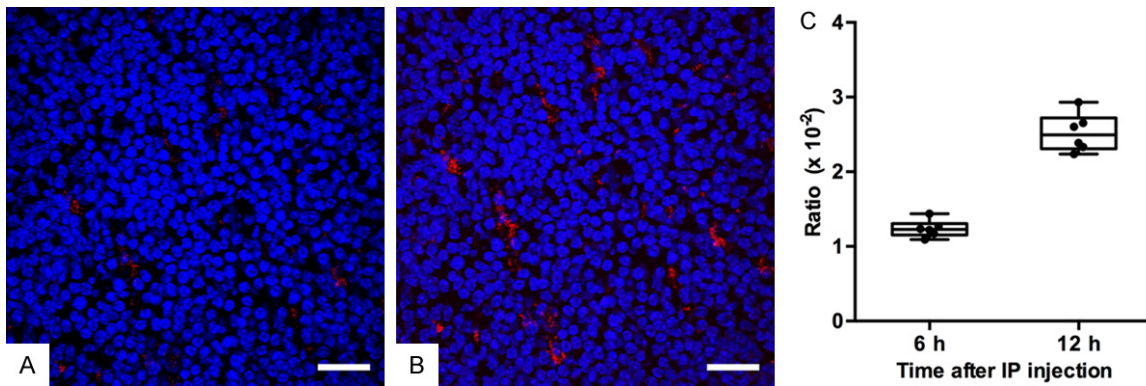


**Figure 3.** The migration of Panc02-pulsed DCs to spleens after IP injection. A. The representative fluorescent microscopy image of spleen harvested 6 h after IP injection (scale bar: 50  $\mu$ m). B. The representative fluorescent microscopy image of spleen harvested 12 h after IP injection (scale bar: 50  $\mu$ m). The PKH26-labeled Panc02-pulsed DCs (red) were detected in spleen tissues (splenic cells, blue). C. A box plot of the ratio of PKH26 positive DCs amount to the total number of cells for spleens harvested 6 h and 12 h after IP injection. The box plot displays the full range of variation (from min to max), and dots indicate individual values. The positive DCs ratio for spleens harvested 12 h after IP injection was significantly higher than the ratio for spleens harvested 6 h after IP injection ( $P = 0.002$ ).

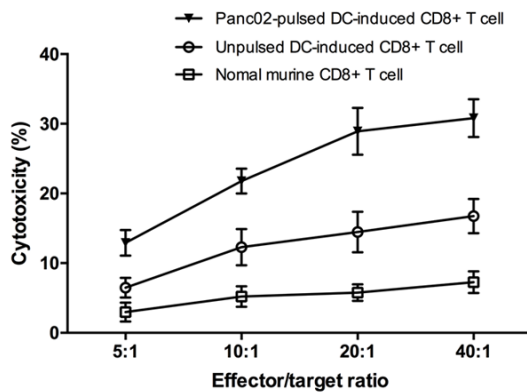


**Figure 4.** Cytotoxicity of Panc02-pulsed DC-induced, unpulsed DC-induced and normal murine CD8+ T cells against Panc02 cells. After three times of IP injection, the CTL response was determined by evaluating the splenic CD8+ T-cell cytotoxicity using LDH assay. Normal murine CD8+ T cells were used as controls. IP injection of Panc02-pulsed DCs induced significantly a higher level of CTL response against Panc02 cells compared to IP injection of unpulsed DCs (E:T = 40:1,  $30.80 \pm 2.71\%$  specific lysis in Panc02-pulsed DC-induced T cell/Panc02 group vs  $16.74 \pm 2.46\%$  specific lysis in unpulsed DC-induced T cell/Panc02 group, or  $7.28 \pm 1.57\%$  specific lysis in normal murine T cell/Panc02 group,  $P < 0.0001$ ).

BMDCs that being cultured *in vitro* for 8 days (Figure 2A) and in BMDCs that being pulsed by Panc02 cells (Figure 2B) both achieved higher than 75%. The maturation of DCs was evaluated by measuring the expression level of maturation surface markers CD80, CD86, H2Db, H2Kb, and MHC class II, indicating that the DCs

after *in vitro* culture were in a mature state that ready to present antigen to T cells (Figure 2).

#### Migration of fluorescence-labeled Panc02-pulsed DCs to spleens via IP injection

In order to track the migration of Panc02-pulsed DCs to spleen, the levels of PKH26-labeled DCs in the spleen were detected by fluorescence microscopy. For spleens harvested 6 h and 12 h after IP injection, the mean ratios of PKH26 positive DCs to the total number of cells were  $(1.24 \pm 0.12) \times 10^{-2}$  and  $(2.52 \pm 0.26) \times 10^{-2}$ , respectively (Figure 3A and 3B). The ratio of positive DCs in spleens harvested 12 h after IP injection was significantly higher than that harvested 6 h after IP injection ( $P = 0.002$ , Figure 3C), indicating the accumulative migration of Panc02-pulsed DCs in spleens.

#### CTL responses induced by IP injection of Panc02-pulsed DCs

To study the anti-tumor toxicity of CTLs that stimulated by Panc02-pulsed DCs, the CD8+ T cells are purified after IP injection of Panc02-pulsed DCs, and its cytotoxicity was evaluated by measuring the LDH that released by co-cultured Panc02 cells. Normal murine CD8+ T cells were used as controls. IP injection of Panc02-pulsed DCs induced a significantly higher level of CTL response against Panc02 cells compared to IP injection of unpulsed DCs or normal murine CD8+ T cells (Figure 4).

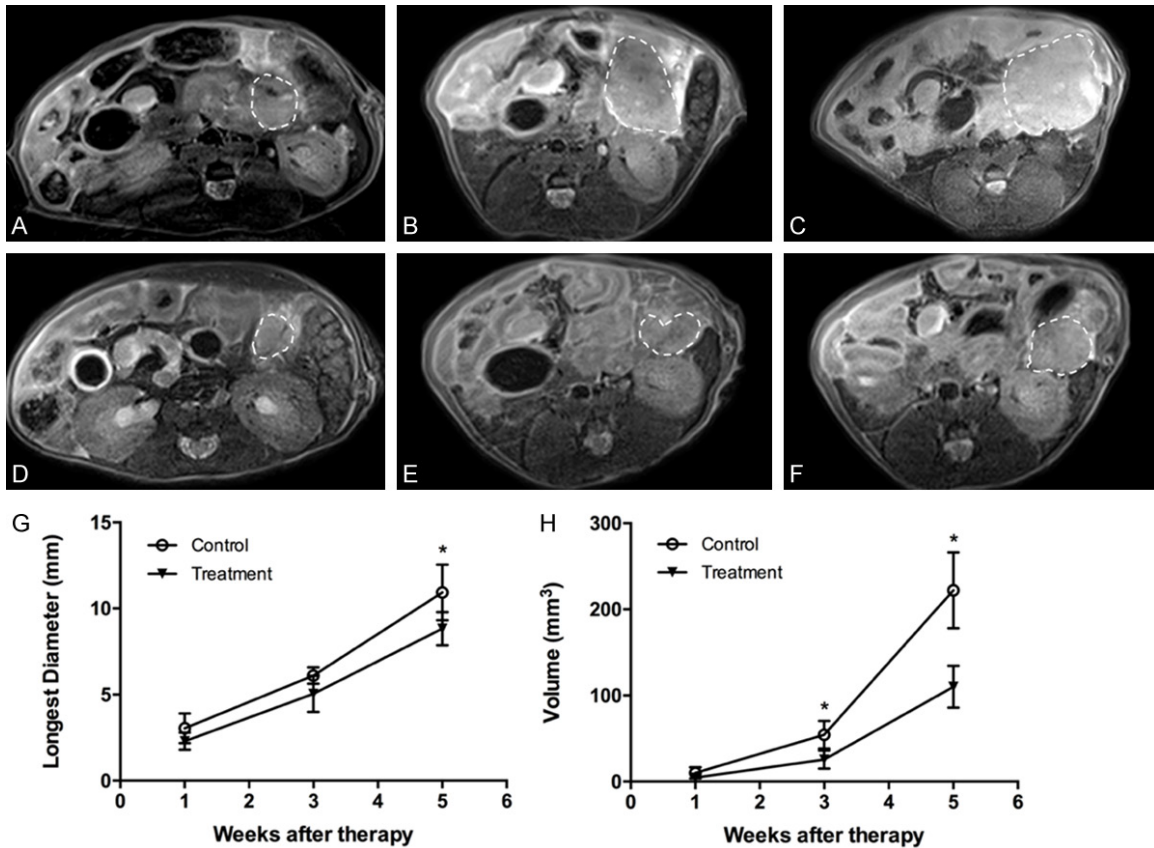


**Figure 5.** *In vivo* tumor size measurement on T2-weighted images. (A-C) Representative axial T2-weighted images of one pancreatic tumor (dash line) in the control group at one week (A), three weeks (B) and five weeks (C) after initiation of treatment. (D-F) Representative axial T2-weighted images of one pancreatic tumor (dash line) in the treatment group at one week (D), three weeks (E) and five weeks (F) after initiation of treatment. (G) Changes of tumor longest diameters for the treatment and control group at different therapeutic time points (error bars indicate SD). There were no significant differences in the longest diameters of the pancreatic tumors between the treatment and the control group one week ( $P = 0.097$ ) and three weeks after initiation of treatment ( $P = 0.500$ ). The longest diameters of the pancreatic tumors in the control group were significantly longer than those in the treatment group five weeks after initiation of treatment ( $P = 0.021$ ). (H) Changes of tumor volumes in the treatment and the control group at different therapeutic time points (error bars indicate SD,  $*P < 0.05$ ). There were no significant differences in tumor volumes between the treatment and the control group one week after initiation of treatment ( $P = 0.076$ ). Tumor volumes in the control group were significantly larger than those in the treatment group three weeks ( $P = 0.004$ ) and five weeks after initiation of treatment ( $P = 0.001$ ).

Therefore, the Panc02-pulsed DCs are capable to trigger strong anti-tumor immunity of CD8+ T cells.

*In vivo tumor size measurement on MR images*

Representative axial T2-weighted images of the pancreatic tumors in the treatment group and control group at different therapeutic time points were shown in **Figure 5A-F**. At one week, three weeks, and five weeks after initiation of treatment, the mean longest diameters were  $2.29 \pm 0.50$  mm,  $5.04 \pm 1.06$  mm, and  $8.83 \pm 0.97$  mm for the treatment group and

$3.04 \pm 0.87$  mm,  $6.10 \pm 0.48$  mm, and  $10.93 \pm 1.62$  mm for the control group respectively (**Figure 5G**). The mean  $\Delta$ diameters were  $6.21 \pm 1.42$  mm for the treatment group and  $7.89 \pm 2.05$  mm for the control group. There were no significant differences in the longest diameters between the treatment and the control group at one week ( $P = 0.097$ ) and three weeks after initiation of treatment ( $P = 0.500$ ). The longest diameter in the control group was significantly longer than that in the treatment group at five weeks after initiation of treatment ( $P = 0.021$ ). However, there was no significant difference in  $\Delta$ diameter between the treatment

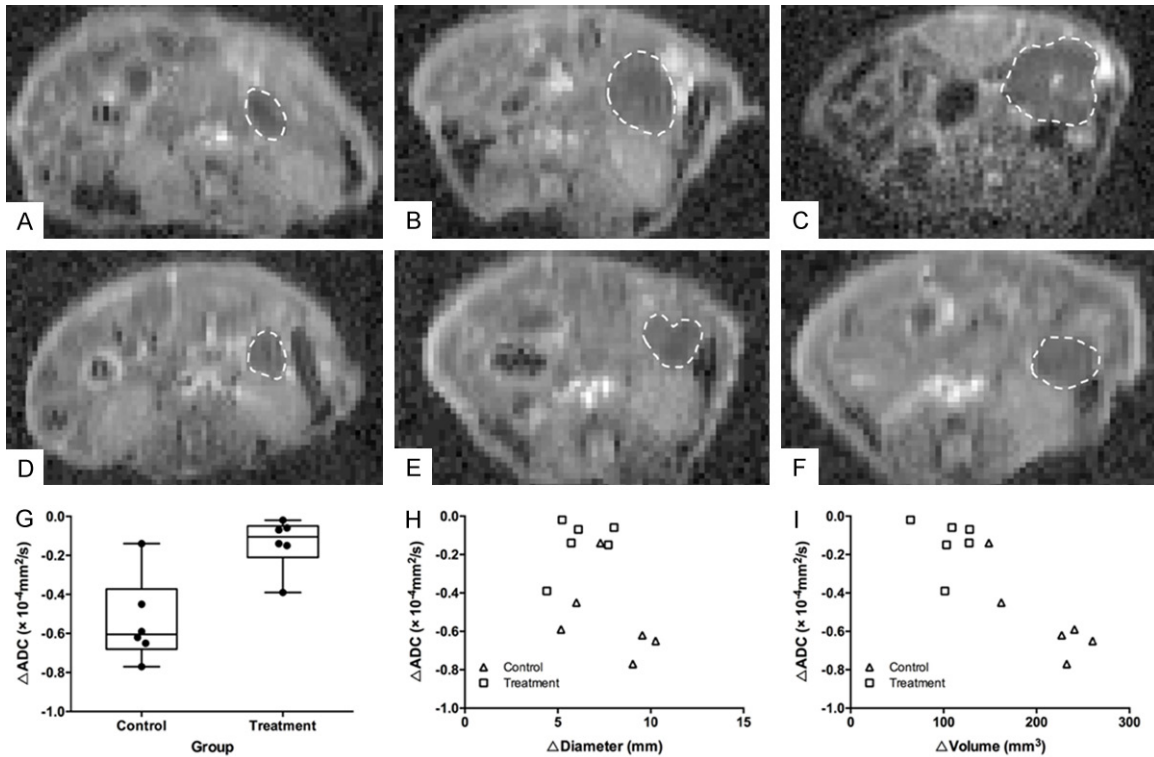


**Figure 6.** ADC measurement on ADC maps of DW-MRI. (A-C) Representative axial ADC maps of one pancreatic tumor (dash line) in the control group at one week (A), three weeks (B) and five weeks (C) after initiation of treatment. (D-F) Representative axial ADC maps of one pancreatic tumor (dash line) in the treatment group at one week (D), three weeks (E) and five weeks (F) after initiation of treatment. (G) A box plot of  $\Delta\text{ADC}$  for the treatment and control group (error bars indicate SD, and dots indicate individual values).  $\Delta\text{ADC}$  of the pancreatic tumor in the treatment group was significantly higher than that in the control group ( $P = 0.004$ ). (H) A scatter plot of the correlation between the change in the longest diameter ( $\Delta\text{diameter}$ ) and the change in ADC ( $\Delta\text{ADC}$ ) after five weeks of treatment. There was no significant correlation between  $\Delta\text{ADC}$  and  $\Delta\text{diameter}$  ( $r = -0.440$ , 95% CI,  $-0.848$  to  $0.509$ ,  $P = 0.152$ ). (I) A scatter plot of the correlation between the change in tumor volume ( $\Delta\text{volume}$ ) and the change in ADC ( $\Delta\text{ADC}$ ) after five weeks of treatment. There was a very strong negative correlation between  $\Delta\text{ADC}$  and  $\Delta\text{volume}$  ( $r = -0.882$ , 95% CI,  $-0.967$  to  $-0.701$ ,  $P < 0.0001$ ).

group and the control group ( $P = 0.129$ ). On the other hand, the tumor volumes have experienced a more dynamic change. The mean tumor volumes were  $4.64 \pm 1.50 \text{ mm}^3$ ,  $25.75 \pm 10.64 \text{ mm}^3$ , and  $110.23 \pm 24.30 \text{ mm}^3$  for the treatment group and  $10.08 \pm 6.58 \text{ mm}^3$ ,  $54.42 \pm 16.02 \text{ mm}^3$ , and  $209.89 \pm 48.69 \text{ mm}^3$  for the control group (Figure 5H). The mean  $\Delta\text{volumes}$  were  $105.59 \pm 23.31 \text{ mm}^3$  for the treatment group and  $211 \pm 45.42 \text{ mm}^3$  for the control group. There was no significant difference in tumor volume between the treatment and the control group at one week after initiation of treatment ( $P = 0.076$ ). Tumor volume in the control group was significantly higher than that in the treatment group at three weeks ( $P = 0.004$ ) and five weeks after initiation of treatment ( $P = 0.001$ ). Also,  $\Delta\text{volume}$  in the treatment group was significant-

ly smaller than that in the control group ( $P < 0.0001$ ).

#### ADC measurement

Representative axial ADC maps of pancreatic tumors in the treatment group and control group at different therapeutic time points were shown in Figure 6A-F. The mean  $\Delta\text{ADCs}$  were  $(-0.14 \pm 0.13) \times 10^{-4} \text{ mm}^2/\text{s}$  for the treatment group and  $(-0.54 \pm 0.22) \times 10^{-4} \text{ mm}^2/\text{s}$  for the control group.  $\Delta\text{ADC}$  in the treatment group was significantly higher than that in the control group ( $P = 0.004$ , Figure 6G). There was no significant correlation between  $\Delta\text{ADC}$  and  $\Delta\text{diameter}$  ( $r = -0.440$ , 95% CI,  $-0.848$  to  $0.509$ ,  $P = 0.152$ , Figure 6H), but a very strong negative correlation between  $\Delta\text{ADC}$  and  $\Delta\text{volume}$  ( $r = -0.882$ , 95% CI,  $-0.967$  to  $-0.701$ ,  $P < 0.0001$ , Figure 6I).

### Discussion

This study provided an effective DC vaccination in a murine PDAC model and successfully monitored the tumor response using ADC measurement. Firstly, our results demonstrated that Panc02-pulsed DC vaccination administered via IP injection induces a tumor-specific CTL response and inhibits tumor growth in a murine PDAC model. Following five weeks of DC vaccination, there was a significant difference in the reduction of tumor ADC between the treatment group and the control group; furthermore, a strong correlation was observed between the change in tumor ADC and the change in tumor volume.

In this study, the Panc02 murine orthotopic pancreatic tumor model was used, which is the animal model mimics both histologic characteristics and biological behaviors of human PDAC, and is ideal for testing the efficacy of DC vaccination in the treatment of PDAC [28, 31, 32]. In this study, apoptotic Panc02 cells generated by UV-B irradiation was used for DC vaccine preparation due to its advantage in antigen loading effectiveness and the capacity of loaded DC in T-cells activation [33]. Our results showed that there was a significant increase in the level of CTL response induced by Panc02-pulsed DCs compared with that induced by unpulsed DCs. As for the administration route of DC vaccine, previous studies have shown that DCs failed to migrate into secondary lymphoid tissues after intratumoral injection, resulting in an inferior capacity to induce adaptive immunity [19, 34]. Lesterhuis et al [18] found that the more laborious and variable intranodal route did not offer an advantage over intradermal route. Although intradermal and subcutaneous injection are the most common routes for vaccination in human clinical trials, low migration rate is the major obstacle that leads to low efficacy [35]. IP injection of DC vaccine in this study is easy to apply, and could deliver a relatively large volume of DC vaccine can be injected at multiple time points. The migration of Panc02-pulsed DCs to the spleen and LNs after IP injection was tested, and a large amount of labeled Panc02-pulsed DCs were observed in those lymphoid organs 12 h after IP injection. Our results indicated that IP injection of DC vaccine could be a potential regimen for pancreatic cancer.

In most mouse PDAC therapeutic studies, tumor size was conventionally assessed by standard dissection techniques with the manual caliper measurements, which could only provide the endpoint data. Compared with the conventional assessment method, MRI could provide noninvasive longitudinal *in vivo* measurements of tumor growth with higher accuracy and repeatability. Besides, the evaluation of cancer therapeutics is conventionally based on measurements of the longest tumor diameters in clinical settings, which are adopted by the revised Response Evaluation Criteria in Solid Tumors guideline (RECIST, version 1.1) [36]. Volume-based size measurements are more effective than one-dimensional or two-dimensional measurements in clinical settings, and the change in tumor volume could be used to predict the overall survival and recurrence-free survival of patients in clinical trials [37]. According to our results, the tumor volume was more sensitive in detecting the changes of tumor size compared to the longest diameter. The results of this study indicated that the measurement of tumor volume could better reflect therapeutic response of DC vaccination in PDAC than that of the longest diameter. Zhang et al [38] showed that quantitative ADC measurement reflected pancreatic tumor microstructure in a rat model. In this study, the value of ADC measurement in monitoring therapeutic response of DC vaccination in PDAC was investigated. The results showed that the reduction of tumor ADC in the treatment group was less than that in the control group. Moreover, the change in tumor ADC was correlated negatively with the change in tumor volume after five weeks of treatment; however, there was no significant correlation between the change in tumor ADC and the change in the longest diameter. These results indicated that ADC measurement could provide a valuable imaging biomarker of therapeutic response to DC vaccination in pancreatic cancer.

The current study had several limitations. First, the sample size of mice pancreatic tumor model was small, and we will enlarge the sample size in the future. Second, MRI examinations were performed at only three time points after initiation of treatment; further investigations will include more time points as well as the over survival rate. Third, we also found that programmed cell death receptor ligand 1 (PD-

L1) was highly expressed in the murine pancreatic tumor model, which was considered to be involved in the mechanism of downregulating the antitumor response [39]. However, we did not explore it in depth in this study. DC vaccination combining with immune checkpoint inhibitors, such as PD-1/PD-L1-inhibitors, is the future direction of our work.

In conclusion, this study demonstrated the efficacy of DC vaccination administered via IP injection for immunotherapy in murine PDAC model, and the feasibility of ADC measurement as an imaging biomarker for assessment of therapeutic responses in immunotherapy.

### Acknowledgements

This study was supported by the National Cancer Institute (grants R01CA209886, R01CA196967) and the development program of Tianjin Municipal Science and Technology Commission (17YFZCSY00870).

### Disclosure of conflict of interest

None.

**Address correspondence to:** Wei Xing, Department of Radiology, The Third Affiliated Hospital of Soochow University, 185 Juqian Street, Changzhou 213003, Jiangsu, China. E-mail: suzhxingwei@suda.edu.cn; Zhuoli Zhang, Robert H. Lurie Comprehensive Cancer Center, Feinberg School of Medicine, Northwestern University, 737 N. Michigan Ave, Chicago 60611, IL, USA. E-mail: zhuoli-zhang@northwestern.edu

### References

- [1] Sarnecka AK, Zagozda M and Durlik M. An overview of genetic changes and risk of pancreatic ductal adenocarcinoma. *J Cancer* 2016; 7: 2045-2051.
- [2] Siegel RL, Miller KD and Jemal A. Cancer statistics, 2015. *CA Cancer J Clin* 2015; 65: 5-29.
- [3] Wysocka O, Kulbacka J and Saczko J. Adjuvant, neoadjuvant, and experimental regimens in overcoming pancreatic ductal adenocarcinoma. *Prz Gastroenterol* 2016; 11: 155-162.
- [4] Adamska A, Domenichini A and Falasca M. Pancreatic ductal adenocarcinoma: current and evolving therapies. *Int J Mol Sci* 2017; 18.
- [5] Garg AD, Vara Perez M, Schaaf M, Agostinis P, Zitvogel L, Kroemer G and Galluzzi L. Trial watch: dendritic cell-based anticancer immunotherapy. *Oncoimmunology* 2017; 6: e1328341.
- [6] Seledtsov VI, Goncharov AG and Seledtsova GV. Clinically feasible approaches to preventing cancer cell-based immunotherapies. *Hum Vaccin Immunother* 2015; 11: 851-869.
- [7] Osada T, Nagaoka K, Takahara M, Yang XY, Liu CX, Guo H, Roy Choudhury K, Hobeika A, Hartman Z, Morse MA and Lyerly HK. Precision cancer immunotherapy: optimizing dendritic cell-based strategies to induce tumor antigen-specific T-cell responses against individual patient tumors. *J Immunother* 2015; 38: 155-164.
- [8] Palucka K and Banchereau J. Cancer immunotherapy via dendritic cells. *Nat Rev Cancer* 2012; 12: 265-277.
- [9] Kalinski P, Muthuswamy R and Urban J. Dendritic cells in cancer immunotherapy: vaccines and combination immunotherapies. *Expert Rev Vaccines* 2013; 12: 285-295.
- [10] Frankenberger B and Schendel DJ. Third generation dendritic cell vaccines for tumor immunotherapy. *Eur J Cell Biol* 2012; 91: 53-58.
- [11] Bol KF, Schreiber G, Gerritsen WR, de Vries IJ and Figdor CG. Dendritic cell-based immunotherapy: state of the art and beyond. *Clin Cancer Res* 2016; 22: 1897-1906.
- [12] Chang JH, Jiang Y and Pillarisetty VG. Role of immune cells in pancreatic cancer from bench to clinical application: an updated review. *Medicine (Baltimore)* 2016; 95: e5541.
- [13] Maccalli C, Parmiani G and Ferrone S. Immunomodulating and immunoresistance properties of cancer-initiating cells: implications for the clinical success of immunotherapy. *Immunol Invest* 2017; 46: 221-238.
- [14] Simon T, Fonteneau JF and Gregoire M. Dendritic cell preparation for immunotherapeutic interventions. *Immunotherapy* 2009; 1: 289-302.
- [15] Galati D and Zanotta S. Hematologic neoplasms: dendritic cells vaccines in motion. *Clin Immunol* 2017; 183: 181-190.
- [16] Jiang H, Wang Q and Sun X. Lymph node targeting strategies to improve vaccination efficacy. *J Control Release* 2017; 267: 47-56.
- [17] Fong L, Brockstedt D, Benike C, Wu L and Engleman EG. Dendritic cells injected via different routes induce immunity in cancer patients. *J Immunol* 2001; 166: 4254-4259.
- [18] Lesterhuis WJ, de Vries IJ, Schreiber G, Lambeck AJ, Aarntzen EH, Jacobs JF, Scharenborg NM, van de Rakt MW, de Boer AJ, Croockewit S, van Rossum MM, Mus R, Oyen WJ, Boerman OC, Lucas S, Adema GJ, Punt CJ and Figdor CG. Route of administration modulates the induction of dendritic cell vaccine-induced antigen-specific T cells in advanced melanoma patients. *Clin Cancer Res* 2011; 17: 5725-5735.
- [19] Guo J, Zhu J, Sheng X, Wang X, Qu L, Han Y, Liu Y, Zhang H, Huo L, Zhang S, Lin B and Yang Z. Intratumoral injection of dendritic cells in combination with local hyperthermia induces systemic antitumor effect in patients with ad-

## MRI monitoring DC vaccine in murine pancreatic cancer models

- vanced melanoma. *Int J Cancer* 2007; 120: 2418-2425.
- [20] Miller FH, Rini NJ and Keppke AL. MRI of adenocarcinoma of the pancreas. *AJR Am J Roentgenol* 2006; 187: W365-374.
- [21] De Robertis R, Tinazzi Martini P, Demozzi E, Dal Corso F, Bassi C, Pederzoli P and D'Onofrio M. Diffusion-weighted imaging of pancreatic cancer. *World J Radiol* 2015; 7: 319-328.
- [22] de Figueiredo EH, Borgonovi AF and Doring TM. Basic concepts of MR imaging, diffusion MR imaging, and diffusion tensor imaging. *Magn Reson Imaging Clin N Am* 2011; 19: 1-22.
- [23] Barral M, Taouli B, Guiu B, Koh DM, Luciani A, Manfredi R, Vilgrain V, Hoeffel C, Kanematsu M and Soyer P. Diffusion-weighted MR imaging of the pancreas: current status and recommendations. *Radiology* 2015; 274: 45-63.
- [24] Thoeny HC and Ross BD. Predicting and monitoring cancer treatment response with diffusion-weighted MRI. *J Magn Reson Imaging* 2010; 32: 2-16.
- [25] De Robertis R, Tinazzi Martini P, Demozzi E, Puntel G, Ortolani S, Cingarlini S, Ruzzenente A, Guglielmi A, Tortora G, Bassi C, Pederzoli P and D'Onofrio M. Prognostication and response assessment in liver and pancreatic tumors: the new imaging. *World J Gastroenterol* 2015; 21: 6794-6808.
- [26] Wilmes LJ, McLaughlin RL, Newitt DC, Singer L, Sinha SP, Proctor E, Wisner DJ, Saritas EU, Kornak J, Shankaranarayanan A, Banerjee S, Jones EF, Joe BN and Hylton NM. High-resolution diffusion-weighted imaging for monitoring breast cancer treatment response. *Acad Radiol* 2013; 20: 581-589.
- [27] Jeon TY, Kim CK, Kim JH, Im GH, Park BK and Lee JH. Assessment of early therapeutic response to sorafenib in renal cell carcinoma xenografts by dynamic contrast-enhanced and diffusion-weighted MR imaging. *Br J Radiol* 2015; 88: 20150163.
- [28] Bauer C, Bauernfeind F, Sterzik A, Orban M, Schnurr M, Lehr HA, Endres S, Eigler A and Dauer M. Dendritic cell-based vaccination combined with gemcitabine increases survival in a murine pancreatic carcinoma model. *Gut* 2007; 56: 1275-1282.
- [29] Jiang YJ, Lee CL, Wang Q, Zhou ZW, Yang F, Jin C and Fu DL. Establishment of an orthotopic pancreatic cancer mouse model: cells suspended and injected in matrigel. *World J Gastroenterol* 2014; 20: 9476-9485.
- [30] Cao MQ, Suo ST, Zhang XB, Zhong YC, Zhuang ZG, Cheng JJ, Chi JC and Xu JR. Entropy of T2-weighted imaging combined with apparent diffusion coefficient in prediction of uterine leiomyoma volume response after uterine artery embolization. *Acad Radiol* 2014; 21: 437-444.
- [31] Collignon A, Perles-Barbacaru AT, Robert S, Silvy F, Martinez E, Crenon I, Germain S, Garcia S, Viola A, Lombardo D, Mas E and Beraud E. A pancreatic tumor-specific biomarker characterized in humans and mice as an immunogenic onco-glycoprotein is efficient in dendritic cell vaccination. *Oncotarget* 2015; 6: 23462-23479.
- [32] Putzer BM, Rodicker F, Hitt MM, Stiewe T and Esche H. Improved treatment of pancreatic cancer by IL-12 and B7.1 costimulation: antitumor efficacy and immunoregulation in a non-immunogenic tumor model. *Mol Ther* 2002; 5: 405-412.
- [33] Inzkirweli N, Guckel B, Sohn C, Wallwiener D, Bastert G and Lindner M. Antigen loading of dendritic cells with apoptotic tumor cell-preparations is superior to that using necrotic cells or tumor lysates. *Anticancer Res* 2007; 27: 2121-2129.
- [34] Eggert AA, Schreurs MW, Boerman OC, Oyen WJ, de Boer AJ, Punt CJ, Figdor CG and Adema GJ. Biodistribution and vaccine efficiency of murine dendritic cells are dependent on the route of administration. *Cancer Res* 1999; 59: 3340-3345.
- [35] Steinman RM and Banchereau J. Taking dendritic cells into medicine. *Nature* 2007; 449: 419-426.
- [36] Eisenhauer EA, Therasse P, Bogaerts J, Schwartz LH, Sargent D, Ford R, Dancey J, Arbuck S, Gwyther S, Mooney M, Rubinstein L, Shankar L, Dodd L, Kaplan R, Lacombe D and Verweij J. New response evaluation criteria in solid tumours: revised RECIST guideline (version 1.1). *Eur J Cancer* 2009; 45: 228-247.
- [37] O'Connor JP, Jackson A, Asselin MC, Buckley DL, Parker GJ and Jayson GC. Quantitative imaging biomarkers in the clinical development of targeted therapeutics: current and future perspectives. *Lancet Oncol* 2008; 9: 766-776.
- [38] Zhang Z, Zheng L, Li W, Gordon AC, Huan Y, Shangguan J, Procissi D, Bentrem DJ and Larson AC. Quantitative functional MRI in a clinical orthotopic model of pancreatic cancer in immunocompetent Lewis rats. *Am J Transl Res* 2015; 7: 1475-1486.
- [39] Birnbaum DJ, Finetti P, Lopresti A, Gilabert M, Poizat F, Turrini O, Raoul JL, Delpero JR, Moutardier V, Birnbaum D, Mamessier E and Bertucci F. Prognostic value of PDL1 expression in pancreatic cancer. *Oncotarget* 2016; 7: 71198-71210.